nature ecology & evolution

ARTICLES

https://doi.org/10.1038/s41559-020-1206-6

Species multidimensional effects explain idiosyncratic responses of communities to environmental change

Andrea Tabi[1]✉, Frank Pennekamp[1], Florian Altermatt[1,2], Roman Alther[1,2], Emanuel A. Fronhofer[1,2,3], Katherine Horgan[1], Elvira Mächler[1,2], Mikael Pontarp[1], Owen L. Petchey[1] and Serguei Saavedra[4]

Environmental change can alter species' abundances within communities consistently; for example, increasing all abundances by the same percentage, or more idiosyncratically. Here, we show how comparing effects of temperature on species grown in isolation and when grown together helps our understanding of how ecological communities more generally respond to environmental change. In particular, we find that the shape of the feasibility domain (the parameter space of carrying capacities compatible with positive species' abundances) helps to explain the composition of experimental microbial communities under changing environmental conditions. First, we introduce a measure to quantify the asymmetry of a community's feasibility domain using the column vectors of the corresponding interaction matrix. These column vectors describe the effects each species has on all other species in the community (hereafter referred to as species' multidimensional effects). We show that as the asymmetry of the feasibility domain increases the relationship between species' abundance when grown together and when grown in isolation weakens. We then show that microbial communities experiencing different temperature environments exhibit patterns consistent with this theory. Specifically, communities at warmer temperatures show relatively more asymmetry; thus, the idiosyncrasy of responses is higher compared with that in communities at cooler temperatures. These results suggest that while species' interactions are typically defined at the pairwise level, multispecies dynamics can be better understood by focusing on the effects of these interactions at the community level.

Environmental conditions vary through space and time and influence whether ecological communities contain a mix of rare and abundant species or are composed of species with similar biomasses (or abundances)[1–3]. Temperature is one such condition but its effects on different species' biomasses are often inconsistent[4]. While some species can increase in biomass and others decrease as a function of temperature, the same species can also decrease or increase in biomass depending on the presence of other species[5–10]. Importantly, understanding how temperature influences species' performance (that is, species' ability to transform external resources into their own biomass) and interactions can provide one approach for explaining such apparently inconsistent effects of temperature[5,11]. Indeed, temperature often alters interactions among plants and animals[5], and species' interactions can even shift from negative to positive in different temperature environments[12–14]. Mathematical analyses and empirical results show that indirect effects of temperature mediated by species' interactions can be large relative to direct ones[15,16]. Hence, understanding how temperature affects species' interactions while at the same time accounting for its effects on species' performances has the potential to explain the varied effects of temperature on community composition.

One approach for understanding and predicting effects of temperature on species' performances and on direct interactions is metabolic theory, in which biological rates scale with body size and temperature[4]. Predictions based on metabolic theory often assume common effects of temperature on all species (that is, one common set of activation energies[17–19], although variation in the distribution of activation energies can be substantial and skewed[20]). Coupled with the relatively large effects of species' interactions, the effect of temperature on species' growth rates has the potential to create the appearance of idiosyncratic community responses under changing environments, and to explain such variation in effects if understood and accounted for. However, how temperature affects the distribution of indirect species' interactions is currently quite unclear, as are the implications of interaction distributions for species' responses to environmental change. These multidimensional and changing factors have impaired our ability to understand or predict the effect of temperature on population and community dynamics[21–23].

Here, we use a structural approach to investigate why temperature inconsistently affects communities as a function of species' interactions[14,24]. This approach applies a geometric perspective to Lotka–Volterra models of population dynamics to quantify the domain in the space of carrying capacities compatible with positive species' abundances (the necessary condition for species' coexistence) as a function of species' interactions—what is called the feasibility domain[24,25]. We focus on the effects of temperature on community composition. We study the effect on community composition by looking at how temperature affects the relationship between species evenness when grown together and the position of species' performance in isolation in the feasibility domain—what we call relative species' performance. We first develop theory to study and measure asymmetry of the feasibility domain using the

[1]Department of Evolutionary Biology and Environmental Studies, University of Zurich, Zurich, Switzerland. [2]Department of Aquatic Ecology, Eawag, Swiss Federal Institute of Aquatic Science and Technology, Dübendorf, Switzerland. [3]ISEM, Université de Montpellier, CNRS, IRD, EPHE, Montpellier, France. [4]Department of Civil and Environmental Engineering, Massachusetts Institute of Technology, Cambridge, MA, USA. ✉e-mail: andrea.tabi@ieu.uzh.ch

Box 1 | | Theoretical framework

Species' performance. Species' performance measures the ability of a species to transform resources into its own biomass. This ability depends both on the species' traits and the species' environment. Species' performance is measured as the carrying capacity (K_i) of each species i in isolation or as the intrinsic growth rate (r_i), depending on the mathematical formalism (see Methods). Hereafter, we define all measures below in terms of carrying capacities.

Feasibility domain. The feasibility domain ($D_F(A)$) is a community's parameter space comprised of the carrying capacities that provide all species' populations with a positive equilibrium as a function of the interaction matrix A. Formally, under Lotka–Volterra dynamics, this feasibility domain corresponds to a convex region defined by $D_F(A) = \left\{\mathbf{K} = N_1^*\mathbf{v}_1 + \cdots + N_S^*\mathbf{v}_S \text{, with } N_1^* > 0, \ldots, N_S^* > 0\right\}$, where N^* are the positive solutions of the system, $\boldsymbol{v}_i$ are the column vectors of the interaction matrix A, and S is the number of species in the community. The column vectors of an interaction matrix can be ecologically interpreted as the multidimensional interaction effects of an individual species on the community. Recall that the elements (a_{ij}) of the interaction matrix (A) define the direct per-capita effect of a species j on the per-capita growth rate of a species i.

Geometric centroid. The geometric centroid of the feasibility domain ($\mathbf{K}_c$) corresponds to the point of maximum species evenness whenever the columns of the interaction matrix have been normalized under any norm[25]. This is true given that in this case, the centroid is equivalent to the centre of mass of a convex object with n vertices all having the same mass. Formally, the centroid is calculated as $\mathbf{K}_c = \frac{1}{S}\mathbf{v}_1 + \cdots + \frac{1}{S}\mathbf{v}_S$, which corresponds to the conditions under which all species have the same biomass at equilibrium.

Species evenness. Species evenness (J) is a description of the distribution of species biomasses within a community. Formally, it is defined as $J(N^*) = -\sum_{i=1}^{S} P_i \log[P_i]/\log(S) \in [0, 1]$, where P_i is the relative biomass of species i at equilibrium (that is, $P_i = N_i^*/\sum_j^S N_j^*$). Note that $J(N^*) = 1$ is the case when all species have the same biomass.

Asymmetry of the feasibility domain. Asymmetry of the feasibility domain ($\phi(A)$) is the variation across all of the column vectors of an interaction matrix A. Note that the column vectors correspond to the spanning vectors of the feasibility domain ($D_F(A)$), implying that $\phi(A)$ represents geometrically the asymmetry of the feasibility domain. Mathematically, it is given by $\phi(A) = \text{s.d.}(||\boldsymbol{v}_1||, \ldots, ||\boldsymbol{v}_S||)$. The higher the value of ϕ(A), the more asymmetrical the feasibility domain.

Relative performance in isolation. Relative performance in isolation (θ) is defined as the distance between the vector of carrying capacities observed in monoculture ($\mathbf{K}$) and the vector of carrying capacities that would result in all species having the same biomass when grown together (that is, the geometric centroid ($\mathbf{K}_c$) of the feasibility domain). Simply put, this measure captures the position of performances in isolation in the feasibility domain. Formally, it is measured as $\theta = \arccos\left(\frac{\mathbf{K}\cdot\mathbf{K}_c}{||\mathbf{K}||\cdot||\mathbf{K}_c||}\right)$. Note that this distance normalizes species' performances by the interaction matrix A, given that the geometric centroid ($\mathbf{K}_c$) is particular to every interaction matrix.

Size of the feasibility domain. The size of the feasibility domain ($\Omega(A)$) is the proportion of the unit sphere of carrying capacities that provide positive equilibria for all populations in the community. That is, the size corresponds to the normalized solid angle generated by the feasibility domain $D_F(A)$, such that it is equal to 1 for the whole unit sphere $\mathbb{B}^S$. The normalized solid angle $\Omega(A)$ is equal to the probability of sampling uniformly a vector of carrying capacities on the unit sphere inside the feasibility domain of an interaction matrix A. Formally, it is calculated as $\Omega(A) = \frac{\text{vol}(D_F(A) \cap \mathbb{B}^S)}{\text{vol}(\mathbb{B}^S)} \in [0, 0.5]$ (ref. [25]).

variability within the column vectors of an interaction matrix. These column vectors describe the effects each species has on all other species in the community (that is, species' multidimensional effects). Then, we hypothesize that increasing the asymmetry of the feasibility domain decouples species evenness when grown together from their relative performances in isolation. We then present empirical results that corroborate this hypothesis, and that also show how and why temperature has idiosyncratic effects on community responses: the idiosyncratic effects are, in fact, expected based on the effect of temperature on the asymmetry of the feasibility domain across communities.

Results

Theoretical results and predictions. To establish our hypothesis, first we define with minimum use of mathematics the measures that are used throughout our study (see Box 1 for mathematical details and Fig. 1 for a conceptual illustration). In our framework, we consider the performance of a species i in isolation as its carrying capacity (K_i). Note that intrinsic growth rates (r_i) can also be used as a measure of species' performance in isolation, depending on the dynamical model under consideration[26,27] (see Methods for further details). Then, we consider that a community of species is characterized by an interaction matrix (A), whose elements (a_{ij}) define the direct per-capita effect of a species j on the per-capita growth rate of a species i. Note that a_{ij} and a_{ji} do not need to be the same. Importantly, the interaction matrix (A) of the community defines the parameter-space region of carrying capacities (or intrinsic growth rates) under which all of the species within the community can have positive biomasses at equilibrium ($N^* > 0$). This parameter-space region is known as the feasibility domain ($D_F(A)$)[28]. The size of the feasibility domain ($\Omega(A)$) can be calculated by the proportion of such region inside the unit sphere (the L2 norm)[25] (see Methods for further details). Larger feasibility domains represent larger differences in species' performances (carrying capacities) that are compatible with feasibility.

Assuming that the dynamics of the community are governed by any model topologically equivalent to a Lotka–Volterra model[29], the location of the vector of carrying capacities observed in monocultures ($\mathbf{K}$) inside the feasibility domain determines the specific distribution of species' biomasses at equilibrium within the community[27]. We quantify this distribution by the species evenness ($J \in [0, 1]$). Thus, we define the position of species' performance in isolation in the feasibility domain (that is, the relative performance of species in isolation, θ) as the distance between the observed vector of carrying capacities in monocultures and the vector that would result in all species having the same biomass when grown together (that is, having maximum species evenness). This distance acts as a normalization factor given that only in the case when species do not

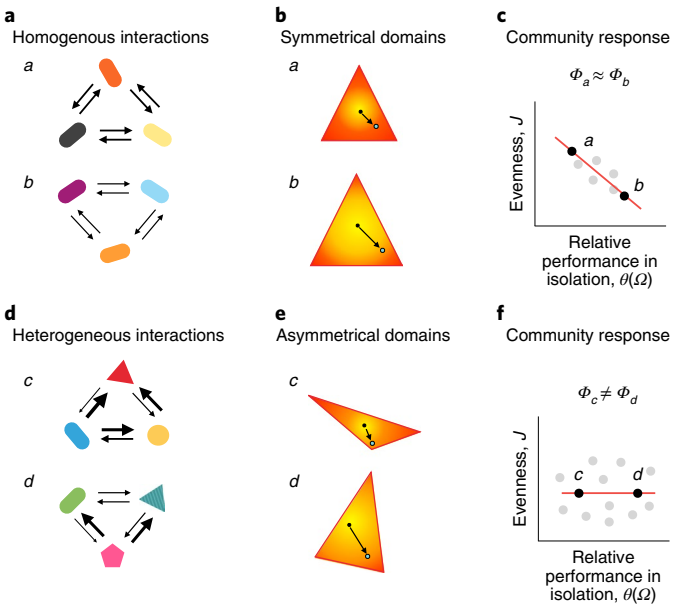

Fig. 1 | Theory relating differences in species' performances in isolation and species evenness when grown together. a–c, A scenario in which different communities have homogeneous interactions (**a**), which can be translated into a symmetrical feasibility domain (**b**), which leads to a strong negative relationship between species evenness when grown together (as a measure of the distribution of species biomasses) and the relative performance in isolation (**c**). **d–f**, A scenario in which communities have heterogeneous interactions (**d**) that result in asymmetrical feasibility domains (**e**), which lead to an unpredictable outcome between species evenness and relative performance in isolation (**f**). **a** and **d** show hypothetical three-species communities in which symbols and colours correspond to different species, while the thickness of arrows represents the direct pairwise interaction strengths. Communities *a* and *b* have less variability in the strength of species' interactions and communities *c* and *d* have more variability. The triangles in **b** and **e** show a two-dimensional simplex (projection) of a three-dimensional cone generated by the column vectors of the interaction matrix. This simplex corresponds to the feasibility domain (that is, the region encapsulating all of the vectors of the carrying capacities **K** (or intrinsic growth rates, ***r***) leading to positive biomasses at equilibrium (see Box 1 for further details). The yellow and red areas inside the feasibility domain represent higher and lower levels of species evenness *J*, respectively. The size and asymmetry of the feasibility domain are represented by Ω and ϕ, respectively. Note that the distribution of species' biomasses has maximum evenness ($J=1$) at the centroid of the feasibility domain (black circle). In contrast, the corner defines the location of perfect unevenness ($J=0$), whereas at the border there is partial unevenness. The blue circle inside a feasibility domain corresponds to the vector of carrying capacities observed in monocultures, **K**. The arrows show the distance between the observed vector **K** (or ***r***) and the centroid of the feasibility domain. We call this distance the relative performance in isolation (θ).

interact, the vector of carrying capacities (**K**) is exactly proportional to the species' biomasses at equilibrium (N^*)[27,30] (see Methods for further details).

Note that the geometric centroid of the feasibility domain corresponds to the vector of carrying capacities leading to all species having the same biomass when grown together[27] (maximum species evenness; $J=1$). This further implies that in order to compare the performance of species across communities, we need to normalize the relative performance (θ) by the size of the feasibility domain as $\theta_n = \theta(0.5 - \Omega(A))$, where 0.5 is the maximum size of any feasibility domain[25] (see Methods for further details). Thus, we estimated the relationship between species evenness when grown together and the relative performance in isolation by the correlation between J and Ω_n.

As we previously mentioned, species' interactions (a_{ij}) can differ in sign as well as strength. Moreover, a community can be characterized by a combination of direct and indirect species interactions[24]. Thus, to provide a well-defined community-level characterization of species' interactions, we calculate the asymmetry ($\phi(A)$) of the feasibility domain. Geometrically, this corresponds to the variability across the column vectors (known as spanning vectors[25]) of the interaction matrix A. Recall that these column vectors can be interpreted as the species' multidimensional effects on the community (see Fig. 1 for a conceptual representation of these equivalences). Formally, $\phi(A) = \text{s.d.}(||\boldsymbol{v}_1||, \ldots, ||\boldsymbol{v}_S||)$, where s.d. corresponds to the standard deviation, $\boldsymbol{v}_i$ is the ith column vector of the interaction matrix A with S species, and $||\cdot||$ corresponds to the L_2 norm.

Based on the definitions above, we now turn to establish our hypothesis. We hypothesize that communities with more symmetrical feasibility domains (that is, small values of $\phi(A)$) generate more homogeneous community responses. Among communities, this leads to relative performance in isolation (θ_n) being tightly correlated with species evenness when grown together (J) (Fig. 1c). Otherwise, differences across communities in the asymmetry of the feasibility domain can increase the idiosyncrasy of community responses (that is, weaken any potential association between θ_n and J) (Fig. 1f). This verbal account of the theory is illustrated with simulations of model communities (see Figs. 2 and 3 and Methods).

How does all of this relate to the effects of temperature on community responses? Based on this theory, we can make contingent hypotheses. If temperature has proportionally similar effects on interaction strengths across communities (that is, if temperature does not affect the asymmetry of the feasibility domains), it will not affect the association of relative performance in isolation and species evenness when grown together (that is, Fig. 1a–c). For example, if temperature doubled the effect on all interactions (including self-regulation), it would not change the shape of the feasibility domain nor its asymmetry. However, if temperature has different effects on interaction strengths (that is, temperature increases the asymmetry of the feasibility domain across communities), it will create idiosyncratic community responses (Fig. 1d–f), weakening the correlation between θ_n and J.

Empirical results. We tested these hypotheses against aquatic microbial communities grown in temperature-controlled environments. Each community contained one, two or three of six species of bacterivorous protists (*Colpidium striatum*, *Dexiostoma campylum*, *Loxocephalus* species, *Paramecium caudatum*, *Spirostomum teres* and *Tetrahymena thermophila*) competing for the same food resource (the bacterium *Serratia fonticola*). Protists, as the most prevalent and diverse organisms on Earth, are essential components of aquatic food webs, providing various ecosystem services and also excellent model organisms due to their fast generation and the ease to control experimental conditions[31]. Furthermore, protist growth rates are strongly temperature dependent[32], which allows for investigating the effects of different environmental manipulations. Communities experienced either a control temperature (15 °C), which the organisms had already experienced for many generations, or one of five elevated constant temperatures (gradually increasing by 2 °C per level).

At the control temperature (15 °C), we observed a negative relationship between relative performance in isolation (θ_n) and species evenness when grown together (J) in two- and three-species communities (Fig. 4), as expected when the feasibility domains are less asymmetrical. These negative relationships persisted at 17, 19 and 21 °C for two-species communities, and at 17 and 19 °C for

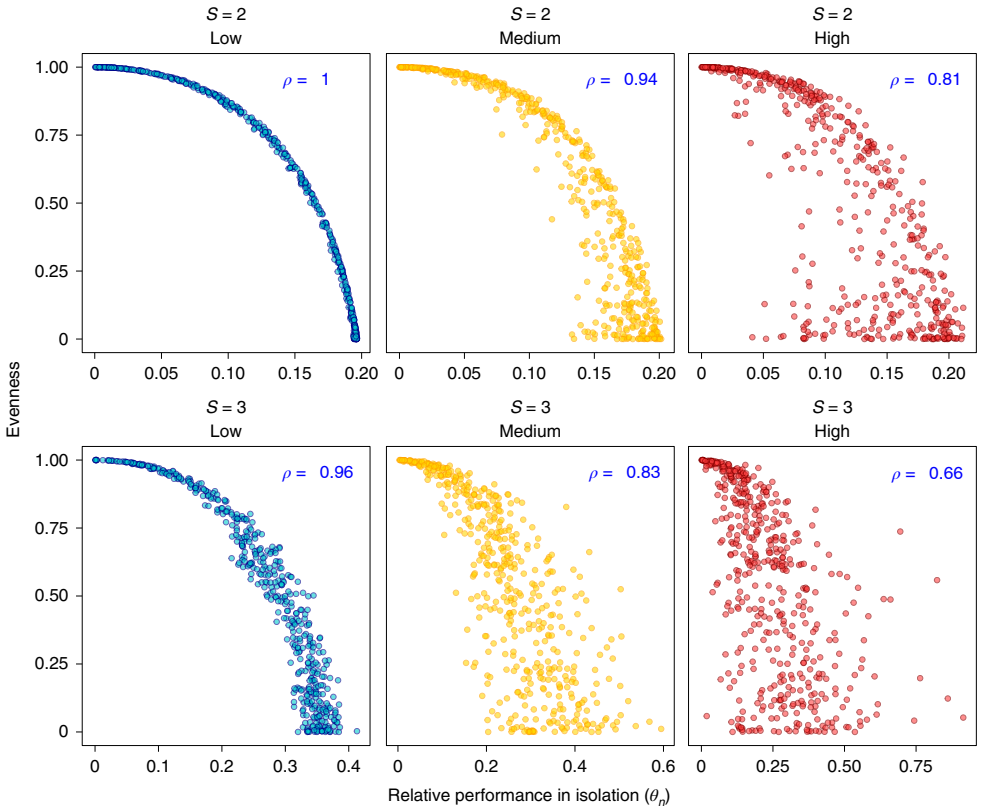

Fig. 2 | Theoretical results. Each point ($n = 500$) represents a different model-generated community with two species (top row) or three species (bottom row) under different asymmetry values of feasibility domains $\phi(A)$ (low = 0.1; medium = 0.5; high = 0.9). We calculated species evenness at equilibrium ($J(N^*)$) and the relative performance in isolation (θ_n). We also report the Spearman's rank correlation coefficients (ρ). All P values were <0.001. See Methods for full details.

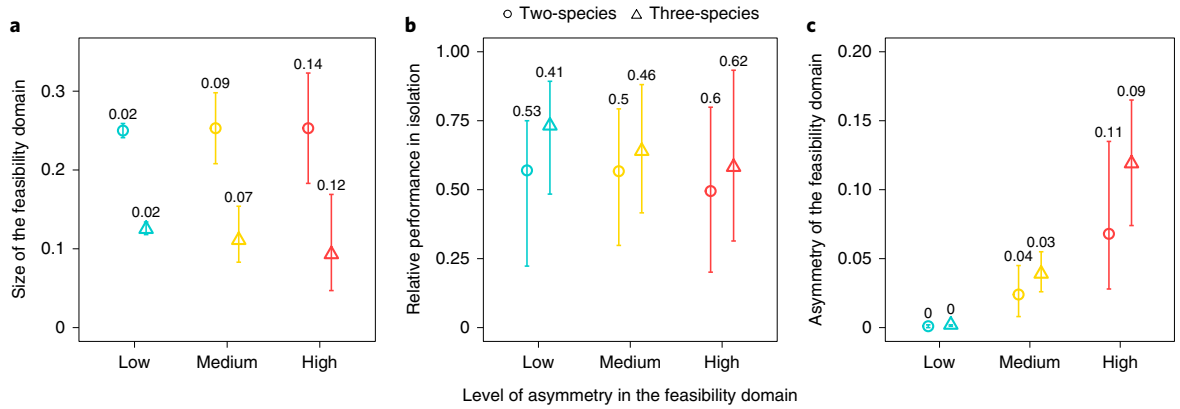

Fig. 3 | Theoretical distribution of structural measures. a–c, Size of the feasibility domain (Ω) (**a**), relative performance in isolation (θ_n) (**b**) and asymmetry of the feasibility domain (ϕ) (**c**) as a function of the level of asymmetry of the feasibility domain. Circles and triangles represent the median values of two- and three-species model-generated communities, respectively. All communities are characterized by randomly generated interaction matrices using a normal distribution with zero mean and different values of standard deviations, which were drawn from a uniform distribution ranging between 0.1, 1 and 10. For each model-generated community and level of standard deviation, we sampled a random vector of carrying capacities $\boldsymbol{K}$ within its size of feasibility domain Ω. The interquartile ranges are shown at the top of each interval. See Methods for full details.

three-species communities. Above these temperatures, there was little evidence of a negative relationship, such that relative performance in isolation did not explain species evenness when grown together. Additionally, we found no systematic directional change in the size of the feasibility domain nor the relative performance across temperatures (Fig. 5a,b). Furthermore, and consistent with the theory, these weaker relationships at higher temperatures were accompanied by more asymmetrical feasibility domains (Fig. 5c). Importantly, these findings reveal that temperature primarily affected species' multidimensional effects on the community, which affected the asymmetry of feasibility domains, which in turn created a weaker relationship between the relative performance (θ_n) and species evenness (J).

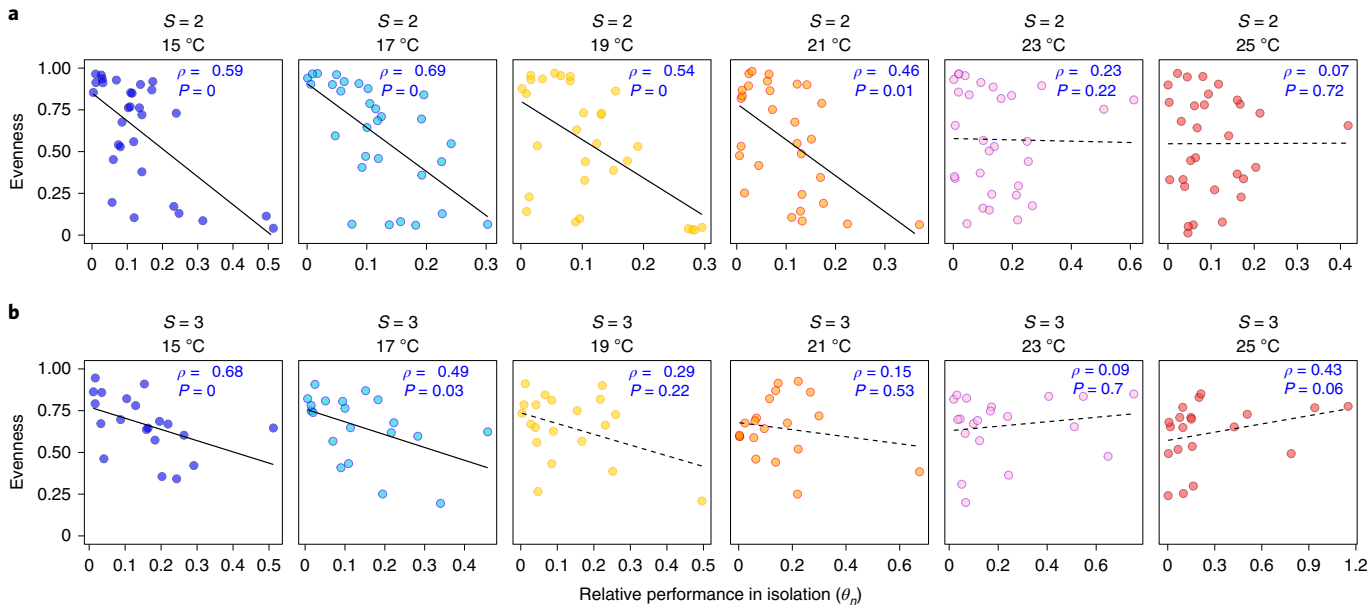

Fig. 4 | Empirical results. a,**b**, Experimental microbial communities formed by different combinations of two (**a**) and three (**b**) protist species under different temperatures. The first column corresponds to communities under a control temperature of 15 °C, whereas the other columns correspond to the communities at elevated constant temperatures. Panels show the relationship between the observed species evenness (J) and the inferred relative performance in isolation (θ_n). Inside the panels, we report the Spearman's rank correlation coefficients (ρ) and corresponding P values among all experimentally generated communities. Solid and dotted lines correspond to slopes that are statistically distinguishable and non-distinguishable from 0, respectively. See Methods for full details.

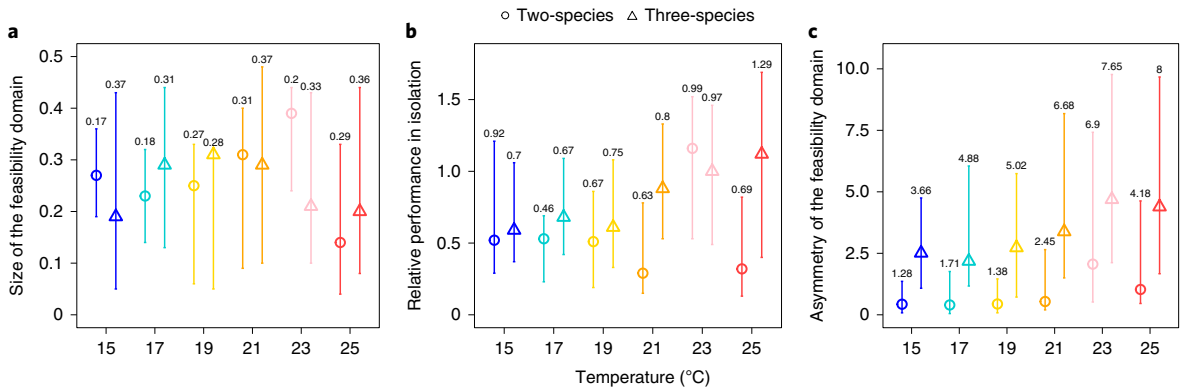

Fig. 5 | Empirical distribution of structural measures across temperatures. a–**c**, Distribution of the size of the feasibility domain (Ω) (**a**), relative performance in isolation (θ_n) (**b**) and asymmetry of the feasibility domain (ϕ) (**c**) across temperatures. Circles (two-species communities) and triangles (three-species communities) denote the median of the corresponding measures calculated from the observations, and the error bars denote the 0.25 and 0.75 quartiles obtained from bootstrapping. The numbers above the error bars show the magnitude of the interquartile range. See Methods for full details.

Discussion

The close match between our empirical findings and our hypotheses corroborates our structural theory of community responses to environmental change; specifically, the relationship between species evenness when grown together and their relative performance when grown in isolation. This confirms that changes in species' performances due to external perturbations insufficiently explain changes in community composition[2]. Instead, we need to also know the shape (asymmetry) of the feasibility domain. Yet, in order to explore the generality of our findings, we need considerably more empirical research examining how temperature and other environmental factors affect species' multidimensional effects across communities.

Importantly, our experiment shows that modest increases in temperature do not disrupt the ability of relative performance in isolation to explain species evenness when grown together, but that larger temperature increases do. The observed diversification of community responses appears to be driven by differences in the asymmetry of feasibility domains. This determines a mapping between composition and structural properties that depends on both responses of species' performance and interactions to environmental change. The increasing asymmetry of feasibility domains with greater temperature change may explain why previous empirical work has shown a lack of unidirectional community responses to warming[7]. Due to the increasing asymmetry of the feasibility domain, species' performance and single pairwise

interactions become a less reliable explanatory variable of species evenness when grown together. These results suggest that while species' interactions are typically defined at the pairwise level, multispecies dynamics can be better understood by focusing on the multidimensional nature of these interactions at the community level.

Our results also corroborate theoretical findings on the link between species evenness and productivity[27]: communities maximize their tolerance to random external perturbation when their compositions are described by a high species evenness and an intermediate level of productivity. This corroboration shows that diversification of species' interactions can be a plausible consequence of different mechanisms responsible for maintaining the tolerance to environmental changes (see Extended Data Figs. 3 and 4). For example, the observed increase in the asymmetry of the feasibility domains is a likely consequence of the multidimensional interaction effect of interspecific variation in thermal sensitivity, differences in thermal range or thermal optima, and differences in adaptation or plasticity to novel temperatures[7]. Importantly, these results suggest that direct and indirect temperature effects are essential for understanding (and potentially predicting) community dynamics. Indirect effects that complexity brings, whereby change in the abundance of a species affects the abundance of another via a third, can be larger compared with direct effects[15]. Our results also suggest that mechanistic models must include the structure of interactions among organisms and not only the direct effects of temperature[33].

While our theoretical results hold under higher diversity and mechanistic models (see Extended Data Fig. 2), in order to move to a general theory of community responses, future experimental work needs to address communities with more than three species and in other ecosystems and environments. Such work should explicitly include comparison of theoretical and experimental work, and involve estimation of responses of species' performances and interactions to environmental change. It could also relax some of the assumptions made in our study, such as temporally invariant performances and interaction strengths, and that species' performances are independent of community composition. It is also important that the effects of temporally varying environmental conditions, including increasing variability and extremes in temperature, are investigated.

Methods

Theory and simulations. For our theoretical investigation, we defined the population dynamics given by the classic Lotka–Volterra model using the *K*-formalism $\dot{N}_i = N_i \frac{r_i}{K_i}(K_i - \sum_{j=1}^{S} a_{ij}N_j)$, where N_i is the biomass of species i, r_i is the intrinsic growth rate of species i, and a_{ij} is the direct per-capita effect of species j on i. The biomasses at equilibrium are calculated as $N^* = A^{-1}\boldsymbol{K}$. Note that the carrying capacity of species i is defined as $K_i = r_i/\alpha_{ii}$. That is, the model can be written in the *r*-formalism as $\dot{N}_i = N_i(r_i - \sum_{j=1}^{S} \alpha_{ij}N_j)$, where $N^* = \alpha^{-1}\boldsymbol{r}$. That is, in the *K*-formalism the carrying capacities modulate the equilibrium points, whereas in the *r*-formalism it is the intrinsic growth rates that determine the equilibrium points. Note, however, that A and α do not have the same units. Here, we used the *K*-formalism to illustrate our work; however, both formalisms are interchangeable for our purposes and their use should depend on data availability.

Recent work[29] has shown that in any model topologically equivalent to the Lotka–Volterra model, the structure of species interactions (embedded in the interaction matrix A) defines a unique relationship between parameters K and the community composition at equilibrium N^* (where $\dot{\boldsymbol{N}} = 0$). This relationship is established by the feasibility domain, which corresponds to a convex region $D_F(A)$ within the parameter space, from which it is possible to link uniquely a set of K_i to a set of feasible (positive) solutions $N_i^* > 0$ (see Box 1 for further details). Formally, this feasibility domain can be written as $D_F(A) = \{K = N_1^*\mathbf{v}_1 + \cdots + N_S^*\mathbf{v}_S, \text{ with } N_1^* > 0, \ldots, N_S^* > 0\}$, where N^* are the positive solutions of the system, $\mathbf{v}_i$ are the column vectors of the interaction matrix A, and S is the number of species in the community. This definition implies that the feasibility domain of an interaction matrix can be geometrically represented as an algebraic cone by normalizing the parameter space under any norm[25]. An algebraic cone is defined as the space spanned by positive linear combinations of S linearly independent vectors $\mathbf{v}_i$. Then, the size of the feasibility domain can be estimated by normalizing the solid angle generated by the feasibility domain, such that it is equal to 1 for the whole unit sphere (using the L2 norm) $\mathbb{B}^S$. This normalized angle can be analytically calculated by $\Omega = \frac{1}{(2\pi)^{S/2}\sqrt{|\det(\alpha)|}} \int \cdots \int_{N^* \geq 0} e^{-\frac{1}{2}N^{*\mathrm{T}}\alpha^{\mathrm{T}}\alpha N^*} \mathrm{d}N^*$, and is computed via a quasi-Monte Carlo method[24,34].

To theoretically investigate the relationship between species evenness and the relative performance in isolation, we generated two- and three-species communities by randomly sampling interaction matrices following a uniform distribution $U[-P, P]$. We used a tuning parameter (P), where the larger the values of P, the larger the asymmetry of the interaction matrix. By including positive and negative interaction coefficients, we ensured comparability with our empirical results. All intra-specific coefficients were set to $a_{ii} = -1$, such that each species saturates to its carrying capacity in isolation. This is an important consideration to take into account given that if one aims to change all pairwise interactions in a community, these values would have to be normalized such that the diagonal elements are always equal to 1. Our results are qualitatively robust to the choice of distribution[34]. We assumed a fully connected interaction structure for both two- and three-species communities (that is, connectance was 1). Parameterizations of K_i inside the feasibility domain were sampled by $K_i = \sum_{j=1}^{S} N_i^*\mathbf{v}_i$, where N_i^* are all values in (0, 1) and $\sum_{i=1}^{S} N_i^* = 1$.

We then calculated the size of the feasibility domain (Ω), the relative performance in isolation θ, the asymmetry of the feasibility domain ϕ, and the species evenness $J(N^*)$ of the randomly generated communities (see Box 1 for definitions). We studied how species evenness $J(N^*)$ changed as a function of the relative performance in isolation θ across different values of asymmetry. Figure 3 confirms that the higher the asymmetry, the higher the variation (measured as the interquartile range) of Ω, θ and ϕ across communities. Additionally, regardless of the asymmetry, Ω and θ were positively correlated, while ϕ was not correlated with any measure. This confirmed that the relative performance in isolation needs to be normalized by the size of the feasibility domain in order to be compared across communities. We normalized it as $\theta_n = \theta(0.5 - \Omega)$ (note that 0.5 is the least upper bound of Ω)[25]. In turn, Fig. 2 confirms that $J(N^*)$ and θ_n are negatively correlated under low asymmetry. However, the higher the asymmetry, the more the relationship between $J(N^*)$ and θ_n weakens, indicating that the relative performance in isolation becomes less and less a reliable indicator of species evenness. Importantly, these differences are driven by the asymmetry of the feasibility domains ϕ. Importantly, the asymmetry is size dependent and can be modulated by the structure of a community; for example, changing the connectance within a community. Yet, the effect of asymmetry on the relationship between relative performance in isolation and species evenness when grown together remains (see Extended Data Fig. 2).

Empirical methods. We factorially manipulated temperature (15, 17, 19, 21, 23 and 25 °C) and community composition (31 unique compositions). Each of the six temperature treatments was controlled by two independent incubators. Previous testing showed low temperature variation of the liquid medium (the set-point temperature varied by 0.1 °C). Measuring temperature with a replicated gradient is recommended to harness the power of a regression design, while still allowing testing for a nonlinear temperature effect[35]. Long-term protist cultures are kept at 15 °C, representing the control temperature to which the species used in the experiment were adapted. Warming usually decreases their carrying capacities but increases growth rates[36]. Experimental communities were created by growing protists to their respective carrying capacities at 20 °C in 1 l bacterized medium. The medium consisted of protist pellets (Carolina Biological Supply) at a concentration of 0.055 g l^{-1} of Chalkley's medium in which the bacterium *S. fonticola* was grown as a common resource for the bactivorous protists. Two autoclaved wheat seeds were added to each bottle for slow nutrient release. Monocultures were initiated at a density of three individuals per ml in a total of 100 ml medium. Communities were initiated with a total of 40 ml protist culture topped up with 60 ml fresh medium (100 ml culture in total). The 40 ml culture was assembled by adding a fixed fraction (that is, 20 ml for two species and 13.33 ml for three species) of each species at their specific carrying capacity, adopting a substitutive design. Each experimental community was cultivated in a 250-ml Duran bottle. Since the number of possible species compositions exceeded the number of feasible experimental units, we used all possible compositions only for the monocultures (six compositions and three replicates) and two-species communities (15 compositions and two replicates). For three-species communities, ten compositions (two replicates) were randomly selected from the set of all possible compositions such that all species occurred the same number of times. This generated a total of 68 experimental units per temperature. Microcosms were sampled 19 times over 36 d to measure community dynamics. To do so, a microcosm was taken out of the incubator and gently stirred to homogenize the culture, and a fixed sample was pipetted into a counting chamber. The height of the sampling chamber was 600 µm and the area filmed was 68.7 mm^2, resulting in 41.2 µl sampled. The counting chamber was covered with a lid and a 5-s video was taken under the microscope. The videos were subsequently processed with the R package BEMOVI[37] to extract morphological and behavioural traits. Individuals in polycultures were classified into species by a random forest classifier trained on trait information obtained from the monoculture data[38]. We derived the biomass of each species by

summing the biovolume of all individuals of a given species in a given community and multiplying biovolume with a constant density equal to water (that is, 1 g cm^{-3}).

Estimation of species interactions. We fitted a topologically equivalent model to the classic Lotka–Volterra model[29] to our observations using the form $\dot{N}_i = N_i \frac{r_i}{K_i}(K_i - \sum_{j=1}^{S} a_{ij} \frac{2N_j}{(1+N_j^{\beta})})$, where β is a tuning parameter that allows us to gradually enter more nonlinear forms of functional responses ($\beta \in [0, 2]$ by step size 0.1). Note that $\beta = 0$ results in a linear functional response. These models were fitted (see an example in Extended Data Fig. 1) to 178 out of 180 combinations (due to early extinctions), where all possible pair combinations were represented (composition (15) × temperature (6) × replicate (2)), and to 120 three-species communities where all possible species pairs were also contained (not all possible three-way combinations). The model parameters (carrying capacities K_i and growth rates r_i) were obtained by fitting logistic growth models to 36 monoculture time series using the following form: $\dot{N}_i = N_i \frac{r_i}{K_i}(K_i - \frac{2N_i}{(1+N_i^{\beta})})$. Growth rates were fitted to the average biomass (of three replicates) at each time point. Carrying capacities were calculated as the median biomass from the observed time series. Fitting was performed with temperature-specific K_i as an environment-dependent parameter for each species i, resulting in temperature-specific r_i values. Using these parameters, the fitting was performed to two- and three-species mixtures as well as to each replicate (see Extended Data Fig. 1 as an example). We used the Nelder–Mead algorithm for optimizing the mean absolute error between observations and predictions.

The model selection was based on maximizing the partial correlation between the fitted and observed time-series data (controlling for time). We selected the simplest model (with the lowest β) from a 5% deviation interval from the highest partial correlation coefficient. This procedure resulted in selection of the linear Lotka–Volterra model in 77% of cases for two-species mixtures and 51% of cases for three-species mixtures. Note that since r_i and K_i are inferred from monocultures, we set $a_{ii} = 1$ for consistency with the K-formalism[26], and all cases yielded topologically similar models to the Lotka–Volterra model[29]. We also tested the robustness of this relationship by bootstrapping the time series 100 times using a uniform sampling within ±1% of each data point and recalculating all of our measures from these slightly perturbed time series. This sensitivity analysis provided appropriate confidence intervals for each variation and regression coefficient given that observational noise is unavoidable.

Reporting Summary. Further information on research design is available in the Nature Research Reporting Summary linked to this article.

Data availability

The experimental data used in this study are available as indicated in ref. [39].

Code availability

Codes for Figs. 2 and 3 are available at https://github.com/MITEcology/NEE_Tabi_et_al_2020.

Received: 23 February 2019; Accepted: 15 April 2020;
Published online: 22 June 2020

References

1. Fukami, T. Historical contingency in community assembly: integrating niches, species pools, and priority effects. *Annu. Rev. Ecol. Evol. Syst.* **46**, 1–23 (2015).
2. Cenci, S., Song, C. & Saavedra, S. Rethinking the importance of the structure of ecological networks under an environment-dependent framework. *Ecol. Evol.* **8**, 6852–6859 (2018).
3. Hutchins, L. W. The bases for temperature zonation in geographical distribution. *Ecol. Monogr.* **17**, 325–335 (1947).
4. Brown, J. H., Gillooly, J. F., Allen, A. P., Savage, V. M. & West, G. B. Toward a metabolic theory of ecology. *Ecology* **85**, 1771–1789 (2004).
5. Tylianakis, J. M., Didham, R. K., Bascompte, J. & Wardle, D. A. Global change and species interactions in terrestrial ecosystems. *Ecol. Lett.* **11**, 1351–1363 (2008).
6. Jiang, L. & Morin, P. J. Temperature-dependent interactions explain unexpected responses to environmental warming in communities of competitors. *J. Anim. Ecol.* **73**, 569–576 (2004).
7. Kordas, R. L., Harley, C. D. G. & O'Connor, M. I. Community ecology in a warming world: the influence of temperature on interspecific interactions in marine systems. *J. Exp. Mar. Biol. Ecol.* **400**, 218–226 (2011).
8. O'Connor, M. I., Piehler, M. F., Leech, D. M., Anton, A. & Bruno, J. F. Warming and resource availability shift food web structure and metabolism. *PLoS Biol.* **7**, e1000178 (2009).
9. Petchey, O. L., McPhearson, P. T., Casey, T. M. & Morin, P. J. Environmental warming alters food-web structure and ecosystem function. *Nature* **402**, 69–72 (1999).
10. Sentis, A., Hemptinne, J.-L. & Brodeur, J. Towards a mechanistic understanding of temperature and enrichment effects on species interaction strength, omnivory and food-web structure. *Ecol. Lett.* **17**, 785–793 (2014).
11. Wootton, J. T. The nature and consequences of indirect effects in ecological communities. *Annu. Rev. Ecol. Syst.* **25**, 443–466 (1994).
12. Bruno, J. F., Stachowicz, J. J. & Bertness, M. D. Inclusion of facilitation into ecological theory. *Trends Ecol. Evol.* **18**, 119–125 (2003).
13. Koltz, A. M., Classen, A. T. & Wright, J. P. Warming reverses top-down effects of predators on belowground ecosystem function in arctic tundra. *Proc. Natl Acad. Sci. USA* **115**, E7541–E7549 (2018).
14. Song, C., Ahn, S. V., Rohr, R. P. & Saavedra, S. Towards a probabilistic understanding about the context-dependency of species interactions. *Trends Ecol. Evol.* **35**, 384–396 (2020).
15. Montoya, J., Woodward, G., Emmerson, M. C. & Solé, R. V. Press perturbations and indirect effects in real food webs. *Ecology* **90**, 2426–2433 (2009).
16. Higashi, M. & Patten, B. C. Dominance of indirect causality in ecosystems. *Am. Nat.* **133**, 288–302 (1989).
17. Binzer, A., Guill, C., Brose, U. & Rall, B. C. The dynamics of food chains under climate change and nutrient enrichment. *Phil. Trans. R. Soc. B* **367**, 2935–2944 (2012).
18. Binzer, A., Guill, C., Rall, B. C. & Brose, U. Interactive effects of warming, eutrophication and size structure: impacts on biodiversity and food-web structure. *Glob. Change Biol.* **22**, 220–227 (2016).
19. Sentis, A., Binzer, A. & Boukal, D. S. Temperature–size responses alter food chain persistence across environmental gradients. *Ecol. Lett.* **20**, 852–862 (2017).
20. Dell, A. I., Pawar, S. & Savage, V. M. Systematic variation in the temperature dependence of physiological and ecological traits. *Proc. Natl Acad. Sci. USA* **108**, 10591–10596 (2011).
21. Davis, A. J., Jenkinson, L. S., Lawton, J. H., Shorrocks, B. & Wood, S. Making mistakes when predicting shifts in species range in response to global warming. *Nature* **391**, 783–786 (1998).
22. Allison, S. D. et al. Microbial abundance and composition influence litter decomposition response to environmental change. *Ecology* **94**, 714–725 (2013).
23. Widder, S. et al. Challenges in microbial ecology: building predictive understanding of community function and dynamics. *ISME J.* **10**, 2557–2568 (2016).
24. Saavedra, S. et al. A structural approach for understanding multispecies coexistence. *Ecol. Monogr.* **87**, 470–486 (2017).
25. Song, C., Rohr, R. P. & Saavedra, S. A guideline to study the feasibility domain of multi-trophic and changing ecological communities. *J. Theor. Biol.* **450**, 30–36 (2018).
26. Vandermeer, J. H. Interspecific competition: a new approach to the classical theory. *Science* **188**, 253–255 (1975).
27. Rohr, R. P. et al. Persist or produce: a community trade-off tuned by species evenness. *Am. Nat.* **188**, 411–422 (2016).
28. Logofet, D. O. *Matrices and Graphs: Stability Problems in Mathematical Ecology* (CRC Press, 1993).
29. Cenci, S. & Saavedra, S. Structural stability of nonlinear population dynamics. *Phys. Rev. E* **97**, 012401 (2018).
30. Saavedra, S., Rohr, R. P., Gilarranz, L. J. & Bascompte, J. How structurally stable are global socioeconomic systems? *J. R. Soc. Interface* **11**, 20140693 (2014).
31. Altermatt, F. et al. Big answers from small worlds: a user's guide for protist microcosms as a model system in ecology and evolution. *Methods Ecol. Evol.* **6**, 218–231 (2015).
32. Fox, J. W. & Morin, P. J. Effects of intra- and interspecific interactions on species responses to environmental change. *J. Anim. Ecol.* **70**, 80–90 (2001).
33. Van der Putten, W. H., Macel, M. & Visser, M. E. Predicting species distribution and abundance responses to climate change: why it is essential to include biotic interactions across trophic levels. *Phil. Trans. R. Soc. B Biol. Sci.* **365**, 2025–2034 (2010).
34. Song, C. & Saavedra, S. Will a small randomly assembled community be feasible and stable? *Ecology* **99**, 743–751 (2017).
35. Cottingham, K. L., Lennon, J. T. & Brown, B. L. Knowing when to draw the line: designing more informative ecological experiments. *Front. Ecol. Environ.* **3**, 145–152 (2005).
36. Leary, D. J. & Petchey, O. L. Testing a biological mechanism of the insurance hypothesis in experimental aquatic communities. *J. Anim. Ecol.* **78**, 1143–1151 (2009).
37. Pennekamp, F., Schtickzelle, N. & Petchey, O. L. BEMOVI, software for extracting behavior and morphology from videos, illustrated with analyses of microbes. *Ecol. Evol.* **5**, 2584–2595 (2015).
38. Pennekamp, F. et al. Dynamic species classification of microorganisms across time, abiotic and biotic environments—a sliding window approach. *PLoS ONE* **12**, e0176682 (2017).
39. Pennekamp, F. et al. Biodiversity increases and decreases ecosystem stability. *Nature* **563**, 109–112 (2018).

Acknowledgements

The University of Zurich Research Priority Programme on Global Change and Biodiversity supported this research. Furthermore, funding came from the Swiss National Science Foundation (grant 31003A_159498 to O.L.P.). Funding was also provided by the Mitsui Chair (S.S.). This is also publication ISEM-2020-075 of the Institut des Sciences de l'Evolution de Montpellier (E.A.F.). We thank Y. Choffat, P. Ganesanandamoorthy, A. Garnier, J. I. Griffiths, S. Greene, T. M. Massie, G. M. Palamara and M. Seymour for help with the data collection. We also thank M. AlAdwani, S. Cenci and C. Song for insightful discussions about this study.

Author contributions

A.T. and S.S. conceived of and wrote the study, and analysed and interpreted the data. O.L.P. took part in the reviewing and editing process. F.P., F.A., R.A., E.A.F., K.H., E.M., M.P. and O.L.P. contributed to the experiment from which data were used as stated in ref. [39].

Competing interests

The authors declare no competing interests.

Additional information

Extended data is available for this paper at https://doi.org/10.1038/s41559-020-1206-6.

Supplementary information is available for this paper at https://doi.org/10.1038/s41559-020-1206-6.

Correspondence and requests for materials should be addressed to A.T.

Reprints and permissions information is available at www.nature.com/reprints.

Publisher's note Springer Nature remains neutral with regard to jurisdictional claims in published maps and institutional affiliations.

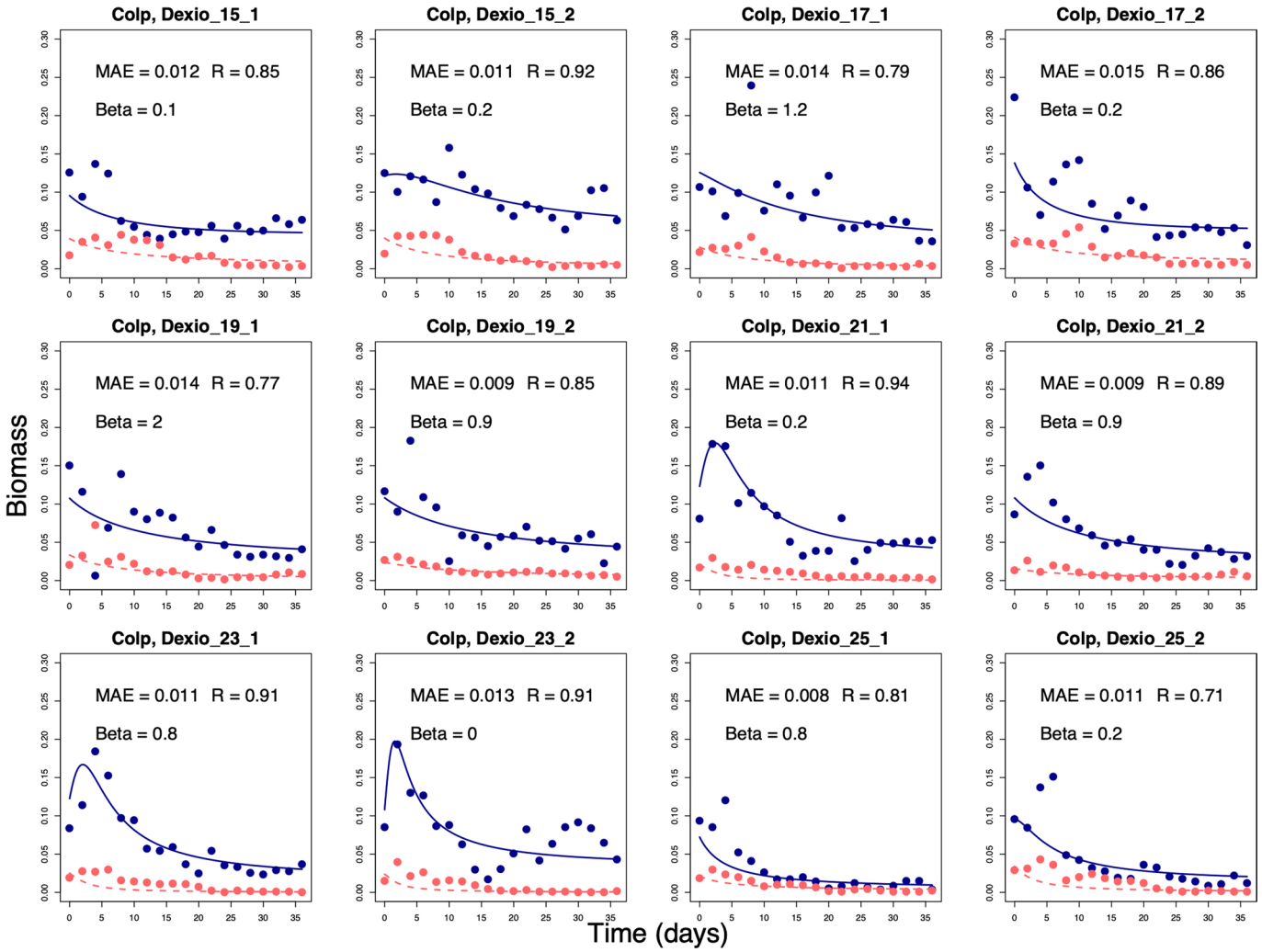

Extended Data Fig. 1 | Example of fitting 2-species LV model across temperature. Illustration using time series of interacting *Colpidium* (blue) and *Dexiostoma* (red) as an example. Each panel shows a different temperature-replicate combination. Dots are the observations and the corresponding lines indicate the prediction of the best fitting model. The mean absolute error (MAE), partial correlation (R) and the tuning parameter (β) of the best fit are also plotted in each graph.

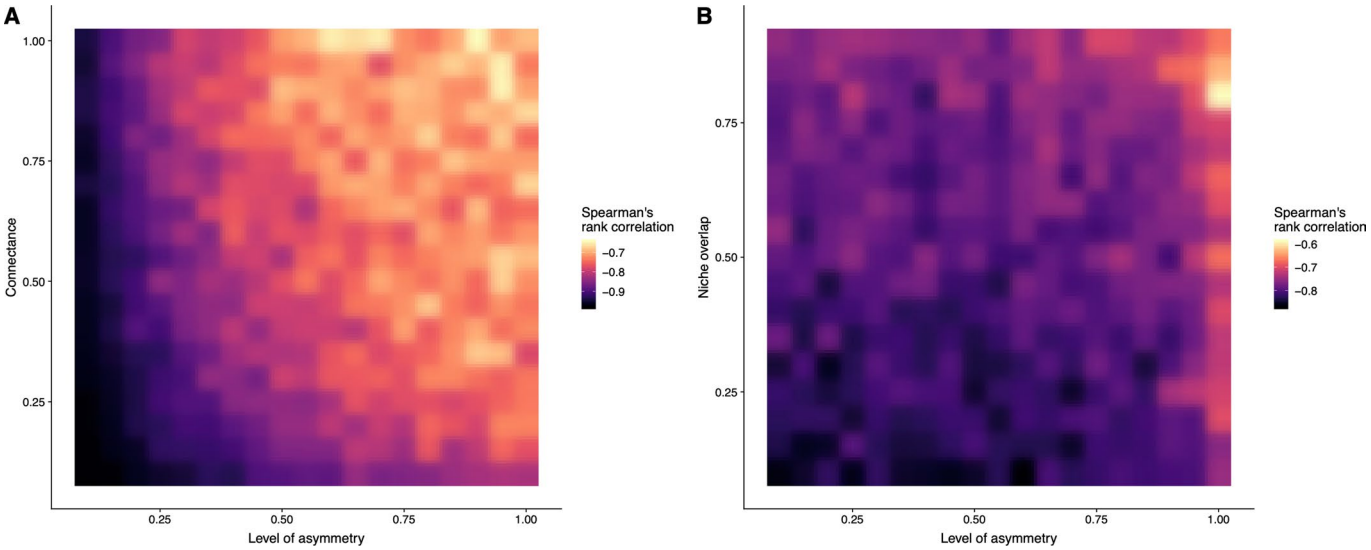

Extended Data Fig. 2 | The effect of connectance, niche overlap and asymmetry on the relationship between species evenness and relative performance in isolation in 10-species communities. Panel (**A**) shows a strong interaction between asymmetry and connectance, that is high asymmetry and connectance leads to the weaker negative relationship (measured as the Spearman's rank correlation) between species evenness and the relative performance in isolation. Connectance is measured as the fraction of non-zero coefficients and modeled following Ref. [34]. Note that the value of asymmetry corresponds to the tuning parameter *P* used in the sampling of the interaction matrix (see Methods). In panel (**B**), we generated the interaction matrices based on a niche framework[27], where all interaction coefficients are negative (competitive). Here, similarly to panel (**A**) high asymmetry and niche overlap lead to the weakest correlation.

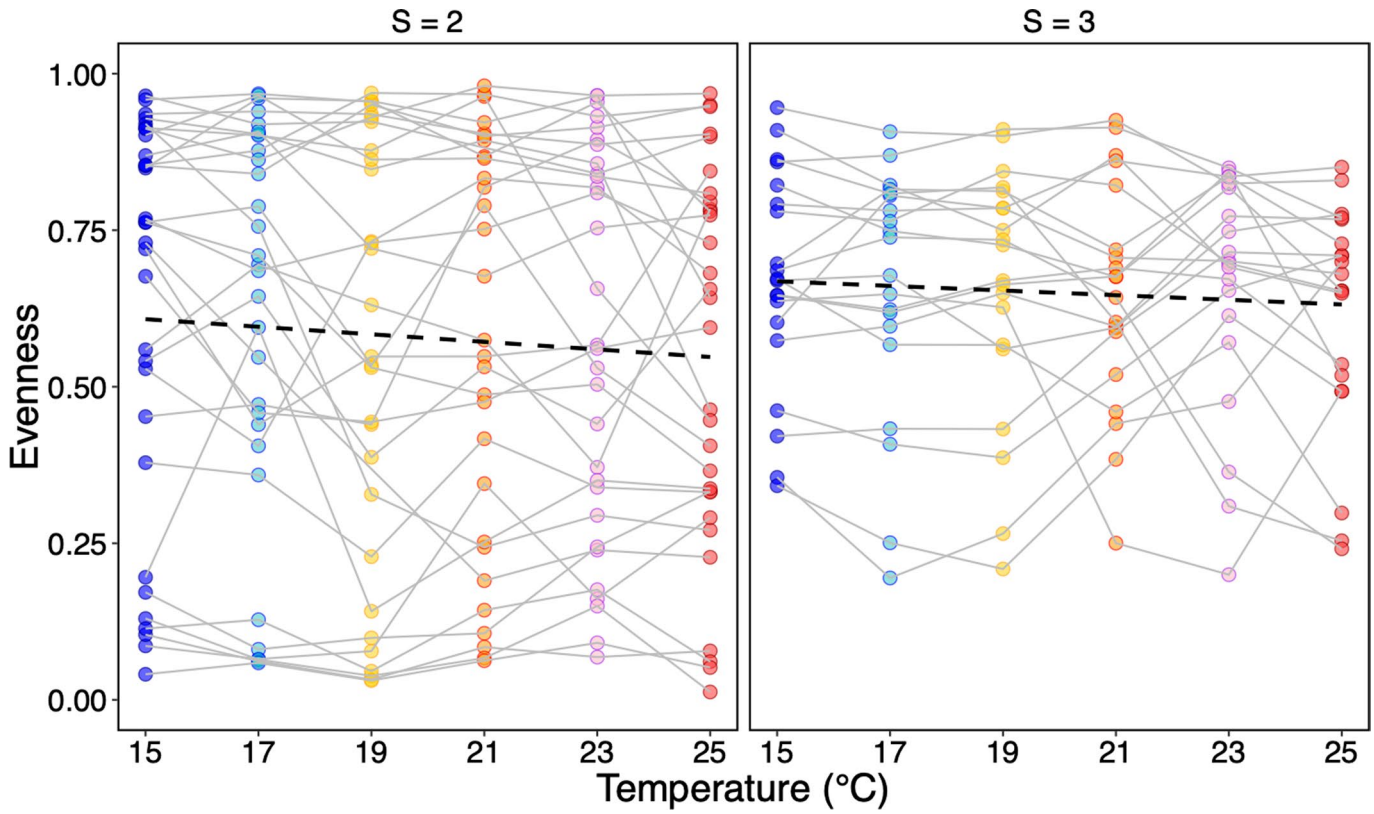

Extended Data Fig. 3 | The relationship between species evenness and temperature empirically measured in 2- and 3-species microbial communities. Species evenness was measured as the median evenness of the time series for each community. There was no statistical relationship found between species evenness and temperature.

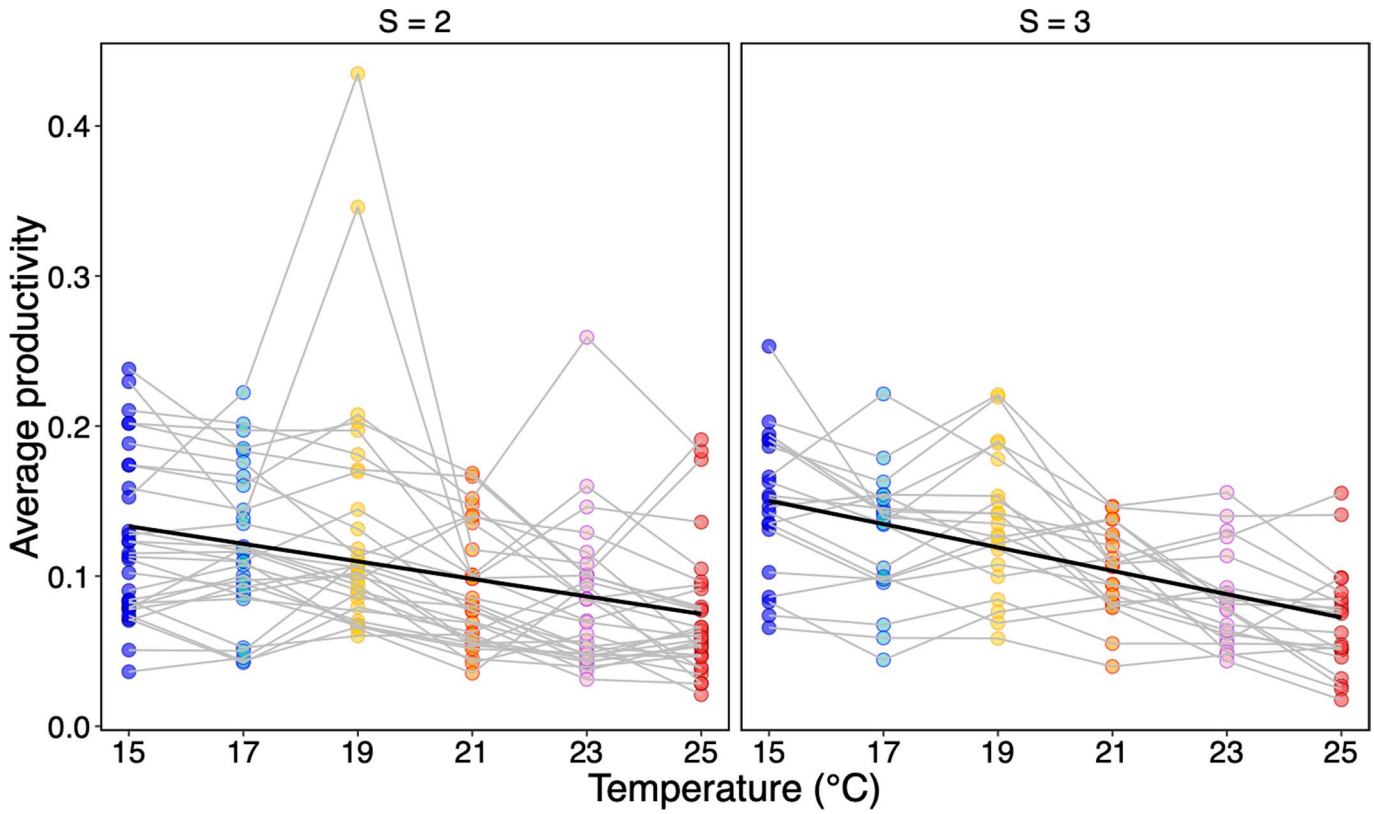

Extended Data Fig. 4 | The relationship between average productivity and temperature empirically measured in 2- and 3-species microbial communities. Average productivity was measured as the median of the time series of total biomass for each community. Average productivity declined with increasing temperature in 2- and 3-species communities as well.

nature research

Corresponding author(s): Andrea Tabi

Last updated by author(s): Apr 2, 2020

Reporting Summary

Nature Research wishes to improve the reproducibility of the work that we publish. This form provides structure for consistency and transparency in reporting. For further information on Nature Research policies, see Authors & Referees and the Editorial Policy Checklist.

Statistics

For all statistical analyses, confirm that the following items are present in the figure legend, table legend, main text, or Methods section.

n/a	Confirmed	
☐	☒	The exact sample size (*n*) for each experimental group/condition, given as a discrete number and unit of measurement
☐	☒	A statement on whether measurements were taken from distinct samples or whether the same sample was measured repeatedly
☐	☒	The statistical test(s) used AND whether they are one- or two-sided *Only common tests should be described solely by name; describe more complex techniques in the Methods section.*
☒	☐	A description of all covariates tested
☒	☐	A description of any assumptions or corrections, such as tests of normality and adjustment for multiple comparisons
☐	☒	A full description of the statistical parameters including central tendency (e.g. means) or other basic estimates (e.g. regression coefficient) AND variation (e.g. standard deviation) or associated estimates of uncertainty (e.g. confidence intervals)
☐	☒	For null hypothesis testing, the test statistic (e.g. *F*, *t*, *r*) with confidence intervals, effect sizes, degrees of freedom and *P* value noted *Give P values as exact values whenever suitable.*
☒	☐	For Bayesian analysis, information on the choice of priors and Markov chain Monte Carlo settings
☒	☐	For hierarchical and complex designs, identification of the appropriate level for tests and full reporting of outcomes
☒	☐	Estimates of effect sizes (e.g. Cohen's *d*, Pearson's *r*), indicating how they were calculated

Our web collection on statistics for biologists contains articles on many of the points above.

Software and code

Policy information about availability of computer code

Data collection	Video processing and analysis was done using the freely available R package BEMOVI (version 1.0.2).
Data analysis	All statistical analyses were done using the statistical computing environment R (version 3.5).

For manuscripts utilizing custom algorithms or software that are central to the research but not yet described in published literature, software must be made available to editors/reviewers. We strongly encourage code deposition in a community repository (e.g. GitHub). See the Nature Research guidelines for submitting code & software for further information.

Data

Policy information about availability of data

All manuscripts must include a data availability statement. This statement should provide the following information, where applicable:

- Accession codes, unique identifiers, or web links for publicly available datasets
- A list of figures that have associated raw data
- A description of any restrictions on data availability

Data and analysis code will be made available in a FAIR compliant repository upon publication.

Field-specific reporting

Please select the one below that is the best fit for your research. If you are not sure, read the appropriate sections before making your selection.

☐ Life sciences ☐ Behavioural & social sciences ☒ Ecological, evolutionary & environmental sciences

For a reference copy of the document with all sections, see nature.com/documents/nr-reporting-summary-flat.pdf

Ecological, evolutionary & environmental sciences study design

All studies must disclose on these points even when the disclosure is negative.

Study description	We factorially manipulated temperature (15, 17, 19, 21, 23 and 25 °C) and community composition (31 unique compositions). Each of the six temperature treatments was controlled by two independent incubators. Since the number of possible species compositions exceeded the number of feasible experimental units, we used all possible compositions only for the monocultures (6 compositions, 3 replicates) and two species communities (15 compositions, 2 replicates). For three species communities, ten compositions (2 replicates) were randomly selected from the set of all possible compositions such that all species occurred the same number of times. This generated a total of 68 experimental units per temperature.
Research sample	We sampled the biomass of bacterivorous ciliate communities with different compositions of the following species: Colpidium striatum, Dexiostoma campylum, Loxocephalus sp., Paramecium caudatum, Spirostomum teres, and Tetrahymena thermophila.
Sampling strategy	For sampling, microcosms were taken out of the incubator, gently stirred to homogenize the culture and a sample was pipetted into a counting chamber. One video was taken per microcosm.
Data collection	We used video sampling techniques to count and measure individual ciliates in all communities.
Timing and spatial scale	Microcosms were sampled 19 times over 36 days to measure community dynamics.
Data exclusions	No data were excluded
Reproducibility	Each treatment combination was successfully replicated at least twice, with replicates being true biological replicates indicating biological variation.
Randomization	Experimental units (jars) were randomly assigned to treatments. During the experiment, experimental units were kept in incubators and positions within incubators changed at random between samplings.
Blinding	No blinding was applied, however, as data was collected via automated video analysis no systematic observer effects are expected.

Did the study involve field work? ☐ Yes ☒ No

Reporting for specific materials, systems and methods

We require information from authors about some types of materials, experimental systems and methods used in many studies. Here, indicate whether each material, system or method listed is relevant to your study. If you are not sure if a list item applies to your research, read the appropriate section before selecting a response.

Materials & experimental systems

n/a	Involved in the study
☒	☐ Antibodies
☒	☐ Eukaryotic cell lines
☒	☐ Palaeontology
☐	☒ Animals and other organisms
☒	☐ Human research participants
☒	☐ Clinical data

Methods

n/a	Involved in the study
☒	☐ ChIP-seq
☒	☐ Flow cytometry
☒	☐ MRI-based neuroimaging

Animals and other organisms

Policy information about studies involving animals; ARRIVE guidelines recommended for reporting animal research

Laboratory animals	We used the following six ciliate species: Colpidium striatum, Dexiostoma campylum, Loxocephalus sp., Paramecium caudatum, Spirostomum teres, and Tetrahymena thermophila. Stocks of these ciliates are kept for many thousands of generations in the lab at 15° C under conditions similar to the monocultures used in the experiment.
Wild animals	The study did not involve wild animals.
Field-collected samples	The study did not involve field-collected samples.
Ethics oversight	No ethical approval was required

Note that full information on the approval of the study protocol must also be provided in the manuscript.